

Dynamical dark energy models and the Λ CDM cosmological model

Gerald Barnert

Departamento de Astronomía, Universidad de Chile, Santiago, Chile

(Dated: July 30, 2021)

Abstract: A breakthrough in modern cosmology was the discovery of an accelerating universe. It indicated the presence of a new dominant component with negative pressure that causes the acceleration: Dark Energy. While a universe dominated by a cosmological constant is appealing because of its simplicity, it poses the problem of the magnitude of the cosmological constant. Because of that, we explore new models of dark energy. We study the cosmology of different dark energy models with dynamical equation of state, at a level of background cosmology, linear matter perturbations and we explore a linear parametrization of the growth index. In order to differentiate between models, we introduce the so-called statefinder parameters r, s , which depend on the third derivative with respect the scale factor. We integrate numerically both background parameters and the matter growth parameters for several dark energy equations of state. We neglect radiation, we use a prior of $\Omega_{m,0} = 0.3$ and we assume a flat geometry of the universe. We show the comparison between the standard cosmological model with equation of state $w = -1$ and different dark energy parametrizations. All models agree with an accelerating universe at the present time. We conclude that $w(z) = w_0 + w_1 \frac{z}{1+z}$ model fits better Λ CDM model and behaves well at high redshift contrary to $w(z) = w_0 + w_1 z$ model that diverges. Oscillating dark energy approaches better Λ CDM at cosmological perturbation level. In the scenario where dark energy and matter components clusters, we found that dark energy perturbations does not affect the evolution of matter perturbations. Assuming some linear parametrization of the growth index, we found a linear behavior of q_0 versus γ'_0 and also that (4, 4) order Padé approximation for w it is enough to reach 5% error between numerical values and its fit. Future observational surveys will provide significant insights into cosmological probes, new measurements of dark energy properties and new information about these parameters may be obtained, leading to a better understanding of dark energy's nature.

1. INTRODUCTION

Current observational data provide strong evidence that we live in a spatially flat universe expanding at an accelerating rate. Einstein's field equations with radiation and non-relativistic matter only cannot lead to accelerating solutions. We need to introduce a new exotic component with a sufficient negative pressure called Dark Energy (DE) that dominates the energy density today. Current constraints indicate that this new component contributes 70% to the total energy density with an equation of state $w = -1$. This has led to think that dark energy is just Einstein's cosmological constant Λ .

The Λ CDM model, based on cold dark matter and a cosmological constant, is the most simple and economical one which is in a very good agreement with observational data. Despite the tremendous observational progress, it suffers from the cosmological constant problem and there are no new insights into the physics behind this mysterious component. These are the basic incentives to explore other possibilities like dynamical equations of state models.

Many dark energy models predict very similar expansion histories and therefore, all of them are still in agreement with current data. In order to discriminate between them, we study new parameters that depends of the third derivative of the cosmic time, the statefinder parameters:

$$r = \frac{\ddot{a}}{aH^3} \quad (1)$$

$$s = \frac{r - 1}{3(q - \frac{1}{2})} \quad (2)$$

where $a(t)$ is the scale factor, which describes the universe expansion, where the present value is $a(t_0) = 1$. $H = \dot{a}/a$ is the Hubble parameter and $q = -\ddot{a}/aH^2$ is the decelerating parameter.

We extend the analysis studying the growth of linear perturbations through the growth function $\delta = \delta\rho/\rho$. Furthermore, we assume some linear parametrization for $\gamma(z)$ and we study its effects on the equation of state parameter and decelerating parameter. The equation of state parameter gives us important information about a Lagrangian description of the universe: depending on whether w is below or above the -1 line, it can be described by a negative (phantom) or positive (quintessence) kinetic term for the scalar field respectively, or crosses the -1 line (quintom). The combination of the equation of state, statefinders parameters and the description of the evolution of matter perturbations can provide significant insight into properties of dark energy.

All these quantities can be computed for a given dark energy model and their values can be extracted from future observations. Observational surveys (Euclid, WFIRST) will help answer questions about the distribution of dark matter in the universe, its expansion history and how the large scale structure of the universe did form through cosmological probes like weak gravitational lensing and baryonic acoustic oscillations. They will allow us to map the dark universe and improve our constraints on dark energy.

Our goal is to study the cosmology of several dark energy models with dynamical equation of state and compare them to the Λ CDM cosmological model.

This work is organized as follows: In §2, we provide a theoretical basis on cosmology, in §3 we show our numer-

ical results and in §4 we summarize our work.

2. THEORETICAL FRAMEWORK

2.1. Background Evolution

The study of the universe starts with the cosmological principle: on large scales, the universe is homogeneous and isotropic. Under this assumption, the metric, which describes the space-time geometry, can be written in the Friedman-Lemaître-Robertson-Walker (FLRW) form:

$$ds^2 = dt^2 - a^2(t) \left[\frac{dr^2}{1 - kr^2} + r^2 (d\theta^2 + \sin^2 \theta d\phi^2) \right] \quad (3)$$

where r, θ and ϕ are the comoving spatial coordinates, t is time and k is the curvature of space. Evidence suggests that $k \approx 0$.

Using the flat FLRW metric in Einstein's equations of general relativity, we obtain the Friedmann equations which describe the evolution of the scale factor:

$$H^2 = \frac{8\pi G\rho}{3} \quad (4)$$

$$\dot{H} = -4\pi G(\rho + p) \quad (5)$$

where G is the Newton's constant, ρ the total energy density and p the total pressure.

We define the critical energy density $\rho_{crit} \equiv 3H^2/8\pi G$. Then, the total energy density can be described relative to its critical value:

$$\Omega = \frac{\rho}{\rho_{crit}} \quad (6)$$

where $\Omega = \Omega_m + \Omega_r + \Omega_{de} = 1$ and the indices m, r, de represent the matter, radiation and dark energy component respectively.

Due to conservation of energy and assuming no interaction between the fluid components, we can derive the continuity equation for each fluid:

$$\dot{\rho} + 3H\rho(1+w) = 0 \quad (7)$$

where w its the equation of state defined as $w \equiv p/\rho$.

The simplest description it is to assume $w = constant$, this is the case of matter $w_m = 0$ and radiation $w_r = 1/3$. The Λ CDM model it is the simplest model, with dark energy equation of state parameter $w = -1$, that can describe the majority of observations of the universe. Constant equations of state do not describe scalar fields dark energy or modified gravity models and therefore, dynamical dark energy models are the most general way to describe dark energy. In this paper, we will assume some parametrization of the dark energy equation of state parameter as a function of redshift $1+z = 1/a$. We can

solve the continuity equation for an arbitrary dark energy equation of state:

$$\rho_{de}(z) = \rho_{de,0} \exp \left(3 \int_0^z \frac{1+w(z')}{1+z'} dz' \right) \quad (8)$$

where $\rho_{de,0}$ it is the present-day energy density of dark energy.

The dimensionless expansion rate of the universe $E(z) = H(z)/H_0$, where H_0 is the present value of the Hubble parameter, can be written as:

$$E^2(z) = \Omega_{m,0}(1+z)^3 + \Omega_{r,0}(1+z)^4 + (1-\Omega_{m,0}-\Omega_{r,0})F(z) \quad (9)$$

where $\Omega_{r,0} = 9 \times 10^{-5}$, $(1-\Omega_{m,0}-\Omega_{r,0}) = \Omega_{de,0}$ and $\Omega_{m,0}, \Omega_{r,0}, \Omega_{de,0}$ are the present values of the normalized densities of matter, radiation and dark energy respectively, and $F(z)$ is given by:

$$F(z) = \exp \left(3 \int_0^z \frac{1+w(z')}{1+z'} dz' \right) \quad (10)$$

For matter and radiation, the normalized energy density is given by:

$$\Omega_m = \frac{\Omega_{m,0}(1+z)^3}{E(z)^2} \quad (11)$$

$$\Omega_r = \frac{\Omega_{r,0}(1+z)^4}{E(z)^2} \quad (12)$$

With all these cosmological equations we derive a new expression for the deceleration and first statefinder parameter:

$$q(z) = -1 + (1+z) \frac{E'(z)}{E(z)} \quad (13)$$

$$r(z) = q(z)(2q(z)+1) + (1+z)q'(z) \quad (14)$$

2.2. Cosmological Perturbations

To explain the large scale structure that we see in the universe, we need to introduce small energy density perturbations $\delta = \delta\rho_m/\rho_m$. The evolution of these fluctuations is given by:

$$\ddot{\delta} + 2H\dot{\delta} - 4\pi G\rho_m\delta = 0 \quad (15)$$

We express the fluctuations and the equation of state in terms of the scale factor, which leads to:

$$\delta'' + \left(\frac{3}{a} + \frac{E'(a)}{E(a)} \right) \delta' = \frac{3}{2} \frac{\Omega_{m,0}}{a^5 E(a)^2} \delta \quad (16)$$

where the prime denotes differentiation with respect the scale factor.

It is useful to introduce new quantities that contains very important sensitivity to dark energy parameters:

$$f \equiv \frac{d \ln \delta}{d \ln a} = \Omega_m^\gamma \quad (17)$$

where f is the growth rate and γ is the growth index. Then, the linear growth of matter perturbations can be written as:

$$\frac{df}{dx} + f^2 + \frac{1}{2} \left(1 - \frac{d \ln \Omega_m}{dx} \right) f = \frac{3}{2} \Omega_m \quad (18)$$

where $x \equiv \ln a$.

All these equations are valid in the regime where $\delta_{de} = 0$. We can extend our analysis studying the evolution of linear perturbations in the regime when matter and DE clusters completely. In this regime, now we have a system of differential equations given by [1]:

$$\delta_m'' + \frac{3}{2a} (1 - w_{de} \Omega_{de}) \delta_m' = \frac{3}{2a^2} (\Omega_m \delta_m + \Omega_{de} \delta_{de}) \quad (19)$$

$$\delta_{de}'' + A \delta_{de}' + B \delta_{de} = \frac{3}{2a^2} (1 + w_{de}) (\Omega_m \delta_m + \Omega_{de} \delta_{de}) \quad (20)$$

where

$$A = \frac{1}{a} \left[-3w_{de} - \frac{aw'_{de}}{1+w_{de}} + \frac{3}{2} (1 - w_{de} \Omega_{de}) \right] \quad (21)$$

$$B = \frac{1}{a^2} \left[-aw'_{de} + \frac{aw'_{de} w_{de}}{1+w_{de}} - \frac{1}{2} w_{de} (1 - 3w_{de} \Omega_{de}) \right] \quad (22)$$

and the initial conditions are given by:

$$\begin{aligned} \delta'_{m_i} &= \frac{\delta_{m_i}}{a_i} \\ \delta_{de_i} &= \frac{1 + w_{de_i}}{1 - 3w_{de_i}} \delta_{m_i} \\ \delta'_{de_i} &= \frac{4w'_{de_i}}{(1 - 3w_{de_i})^2} \delta_{m_i} + \frac{1 + w_{de_i}}{1 - 3w_{de_i}} \delta'_{m_i} \end{aligned} \quad (23)$$

2.3. Equation of state parametrizations

Being the ratio of pressure to energy density, the equation of state parameter w provides a useful phenomenological description of dark energy. A general function of redshift $w(z)$ would be the most general way to describe dark energy. In this section we present different dark energy models where the equation of state evolves with the universe. We do not know the physics behind dark energy and therefore, we explore models beyond the cosmological constant using explicit parametrization of the equation of state parameter $w(z)$. All of these functions have many free parameters that we need to measure. Even measuring a few is challenging and therefore the most popular models contain only a few. We use free parameter values computed in previous works [2, 3]. Table 1 shows the best fit parameters for each model using SNIa data, BAO, CMB and gravitational lensing.

2.3.1. Λ CDM model

Is the simplest model characterized by a single parameter with equation of state $w = -1$. The dimensionless Hubble parameter is given by:

$$E^2(z) = \Omega_{m,0}(1+z)^3 + 1 - \Omega_{m,0} \quad (24)$$

2.3.2. Linear Ansatz

First order Taylor expansion of $w(z)$ around zero:

$$w(z) = w_0 + w_1 z \quad (25)$$

which leads to the dimensionless Hubble parameter:

$$\begin{aligned} E^2(z) &= \Omega_{m,0}(1+z)^3 + (1 - \Omega_{m,0}) \\ &\times (1+z)^{3(1+w_0-w_1)} e^{3w_1 z} \end{aligned} \quad (26)$$

2.3.3. Linder Ansatz

This model behaves like Linear model at low redshift but it is bounded at high redshift:

$$w(z) = w_0 + w_1 \frac{z}{1+z} \quad (27)$$

which leads to the dimensionless Hubble parameter:

$$\begin{aligned} E^2(z) &= \Omega_{m,0}(1+z)^3 + (1 - \Omega_{m,0}) \\ &\times (1+z)^{3(1+w_0+w_1)} e^{3w_1(\frac{1}{1+z}-1)} \end{aligned} \quad (28)$$

2.3.4. Oscillating Ansatz

We can also start directly from the dimensionless Hubble parameter:

$$\begin{aligned} E^2(z) &= \Omega_{m,0}(1+z)^3 + a_1 \cos(a_2 z^2 + a_3) \\ &+ (1 - a_1 \cos(a_3) - \Omega_{m,0}) \end{aligned} \quad (29)$$

2.3.5. Oscillating Dark Energy models

We present two oscillatory equation of state parameters used in [3]:

$$w_1(z) = w_0 + b[1 - \cos[\ln(1+z)]] \quad (30)$$

$$w_2(z) = w_0 + b \sin[\ln(1+z)] \quad (31)$$

which leads to the usual dimensionless Hubble parameter (Eq. 9), where

$$F_1(z) = (1+z)^{3(1+b+w_0)} e^{-3b \sin(\ln(1+z))} \quad (32)$$

$$F_2(z) = (1+z)^{3(1+w_0)} e^{3b(1-\cos \ln(1+z))} \quad (33)$$

2.4. Growth index parametrization

In this section we explore the connection between the growth index γ , equation of state parameter w and the deceleration parameter q . The gamma index is intrinsically related to the growth of linear perturbations (Eq. 17) and it is a way to discriminate between dark energy models.

Let us assume that the solution for δ leads to:

$$\gamma(z) \approx \gamma_0 + \gamma'_0 z \quad (34)$$

which can be viewed as a first Taylor expansion around zero, where the parameter values are constrained by [4]: $0.5 < \gamma_0 < 0.6$ and $-0.05 < \gamma'_0 < 0.05$.

2.4.1. Padé Parametrization

Given a function $f(x)$, the Padé approximate of order (m, n) is given by:

$$f(x) = \frac{a_0 + a_1 x + a_2 x^2 + \dots + a_n x^n}{b_0 + b_1 x + b_2 x^2 + \dots + b_m x^m} \quad (35)$$

where $m \geq 0$, $n \geq 1$ and a_i, b_i are constants.

To compute the equation of state parameter w from F , we differentiate Eq. (10), which leads to:

$$w(z) = \frac{F'(z)}{F(z)} \frac{1}{3}(1+z) - 1 \quad (36)$$

Then, we can fit a n order polynomial to the numerical solution obtained for F , which corresponds to a Padé approximation of order (n, n) for the equation of state parameter w .

3. RESULTS

In this section we show our results for several dark energy models with a given parametrization. Since we are not interested in Cosmic Microwave Background anisotropies, we integrate the equations numerically using *Mathematica*.

3.1. Background Evolution

In FIG. 1 we show the equation of state parameter w for models introduced in § 2.3. We see that only the first oscillating dark energy model evolves in the phantom regime, while all others models evolves in the quintessence regime and no w parametrization crosses the $w = -1$ line.

We compute all the quantities of interest using the parameters shown in Table 1 for the first 4 equations of state parametrizations. The parameters are the results of fitting cosmological data to several cosmological models

and $H(z)$ ansatze, assuming flat geometry of the universe and a prior of $\Omega_{m,0} = 0.3$. We adopt these assumptions. Furthermore, we can neglect the $\Omega_{r,0}$ term studying times after matter-radiation equality $z \approx 10^3$, but dark energy shows a very different behavior once radiation became smaller. In the standard cosmological model, dark energy density overcomes matter density at recent times (FIG. 2). This behavior can be seen in FIG. 4, that shows the deceleration parameter versus redshift. All models agree with an accelerating universe at the present time. We can see that Linear and Oscillating Ansatz models deviates significantly from the Λ CDM model. The first and second statefinder parameters r and s versus redshift are shown in FIG. 5 and 6 for all four models. We see in FIG. 5 that Linder model approaches Λ CDM model, while Linear and OA models deviates at high redshift. In FIG. 6 we see more difference between Linder and Λ CDM model, while Linear and OA models diverges at $z \sim 0.5$.

3.2. Cosmological perturbations

For matter perturbations, first we study the evolution of linear perturbations in the scenario where DE does not cluster. We integrate equation (16) from $a \sim 0.01$ to the present time. To set the appropriate initial conditions, we solve equation (16) analytically in a matter dominated universe, finding that $\delta \propto a$. We see in FIG. 7 that Linear model has an extreme behavior at low scale factor, which is to be expected since Linear model its a Taylor expansion valid at low redshift, while OA model approaches Λ CDM model at high redshift. We show the solution of f and γ in FIG. 8 and FIG. 9. We see that the growth rate increases with redshift for all models. The growth index for the Λ CDM model is $\gamma \approx 0.55$, while the OA model approaches better to the Λ CDM model.

In the scenario when DE clusters with matter, we solve the system of differential equations (Eq. 19 and 20). We set $a_i = 10^{-4}$ and $\delta_{m,i} = 1.5 \times 10^{-5}$. Linear and Linder models do not behave well at high redshift, and the Oscillating Ansatz crosses the $w = -1$ line several times so we found divergences solving the equation for linear perturbations. Hence, we choose two Oscillating Dark Energy models (§2.3.5) and the results are shown in FIG. 10. Perturbations grow as the scale factor increases and we see that despite δ_{de} evolves differently, their impact on δ_m is identical.

3.3. Growth index parametrization

We solve Eq. (18) for $F(a)$, given the growth index parametrization, with the appropriate initial condition $F(a_0) = 1$, and compute the equation of state parameter w and the deceleration parameter q . We explore different combinations of $\gamma_0 = \{0.53, 0.55, 0.57, 0.59\}$, $\gamma'_0 = \{-0.04, -0.02, 0.02, 0.04\}$. In FIG. 11 we show the results for the equations of state parameter w . We see

TABLE I. Best fit parameters for Linder, Linear, OA and ODE models.

Models	Best Fit Parameters
Linder	$w_0 = -1.29, w_1 = 2.84$
Linear	$w_0 = -1.25, w_1 = 1.97$
Oscilatting Ansatz	$a_1 = -3.36, a_2 = 2.12, a_3 = -0.06\pi$
ODE model 1	$w_0 = -1.0267, b = -0.2601$
ODE model 2	$w_0 = -1.0517, b = 0.0113$

an interesting pattern which is that all solutions intersect at the same point. The redshift corresponding to the intersections increases as γ_0 increases. Furthermore, as γ'_0 increases, the value of the equation of state parameter today w_0 increases as well. Covering all possible combinations, we found equations of state parameters that keeps in the phantom or quintessence regime, others that are quintom models that crosses the -1 line at low redshift and others that will eventually cross the line at high redshift. We can see approximately the same behavior for the deceleration parameter q in FIG. 12. In this case, for $\gamma_0 = 0.53$ we see two intersections and the redshift corresponding to the other intersections almost agree with the equation of state parameter case. We also see that the deceleration parameter today q_0 decreases as γ'_0 increases. This behavior can be seen in FIG. 13, where we plot q_0 versus γ'_0 . We found that q_0 not only decreases as γ'_0 , but fits very well a linear function which its slope decreases with γ_0 . We can also see that the allowed range for γ_0 can lead to either decelerating or accelerating universe at present time.

The black-dashed line in FIG. 13 represent the range of $q_0 = 0.5 \pm 0.08$ constrained by [5] using standard sirens. Then, we can constrain γ_0 and γ'_0 . Using these results, we pick $\gamma_0 = 0.55, \gamma'_0 = -0.04$. We can see in FIG. 11 and 12 that these values leads to a quintom equation of state and it is below -1 at the present time, while the deceleration parameter is negative at the present time, but at redshift $z > 1$ became positive. Then, we solve Eq. (18) for $F(z)$ with these parameters values and we fit a n order polynomial to $F(a)$, where $n = \{1, 2, 3, 4\}$, which is equivalent to do a (n, n) Padé parametrization (Eq. 35) for the equation of state parameter w (Eq. 36). Then, we compute $w(z)$ with the best fit for $F(a)$ for a linear, quadratic, cubic and quartic polynomial function and we compare it with the numerical value (FIG. 14). In the bottom panels of each Figure we can see the relative error between the fit and the numerical value, where the gray-dashed lines represent 5% error. We see that the linear approximation reaches 50% of error, while the quadratic and cubic approximations keep in the 5% range but fails at $z = 1$. This indicates that we need to go at least (4, 4) order for the Padé parametrization.

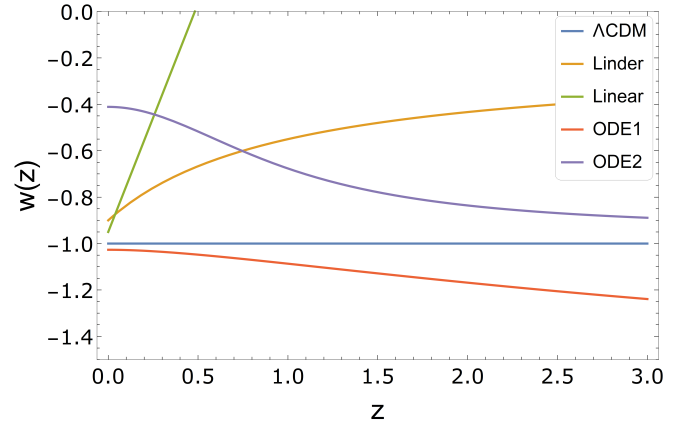


FIG. 1. Equation of state parameter versus redshift for the Λ CDM (blue line), Linder (orange line), Linear (green line), Oscillating Dark Energy 1 (red line) and Oscillating Dark Energy 2 (purple line) models.

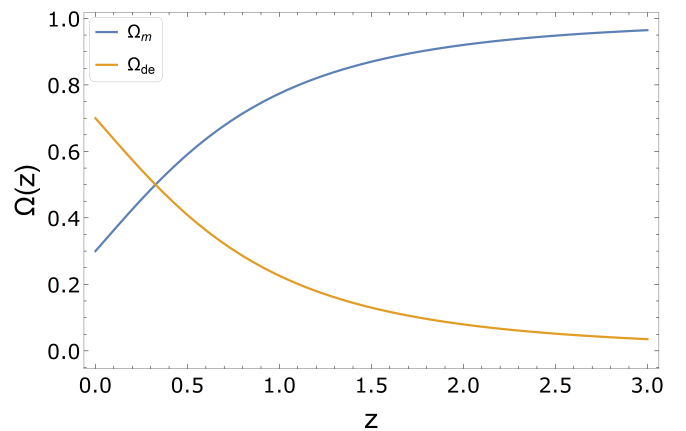


FIG. 2. Omega matter (blue line) and Omega dark energy (orange line) versus redshift for the Λ CDM model.

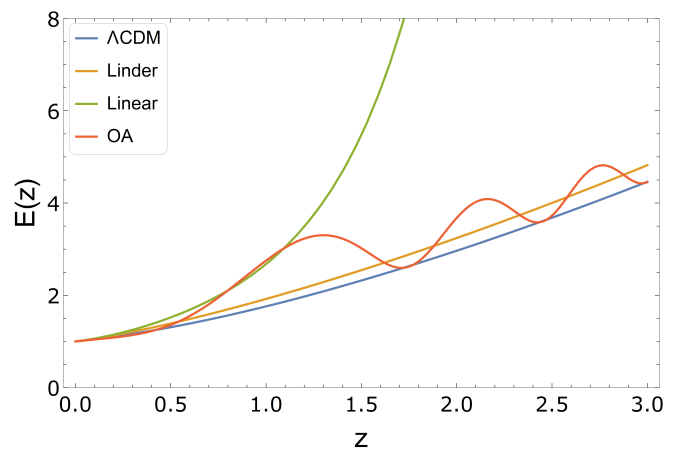


FIG. 3. Dimensionless Hubble parameter versus redshift for the Λ CDM (blue line), Linder (orange line), Linear (green line) and Oscillating Ansatz (red line) models.

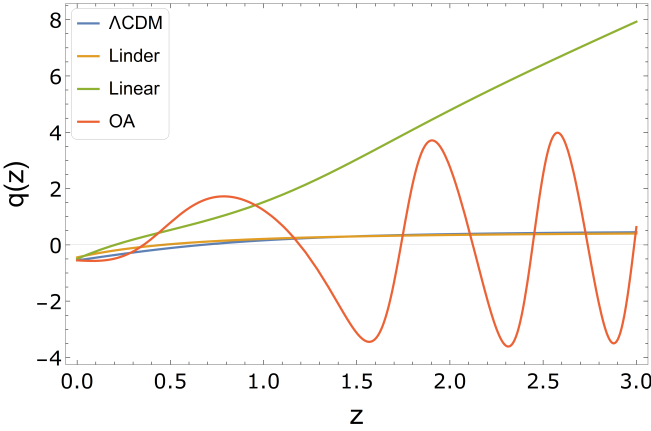


FIG. 4. Deceleration parameter versus redshift for the Λ CDM (blue line), Linder (orange line), Linear (green line) and Oscillating Ansatz (red line) models.

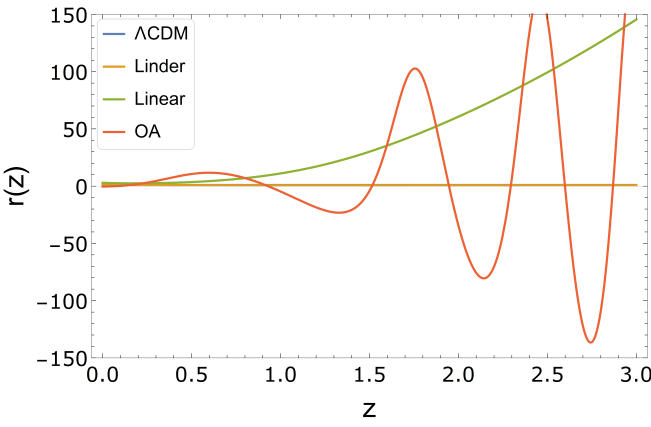


FIG. 5. First statefinder parameter versus redshift for the Λ CDM (blue line), Linder (orange line), Linear (green line) and Oscillating Ansatz (red line) models.

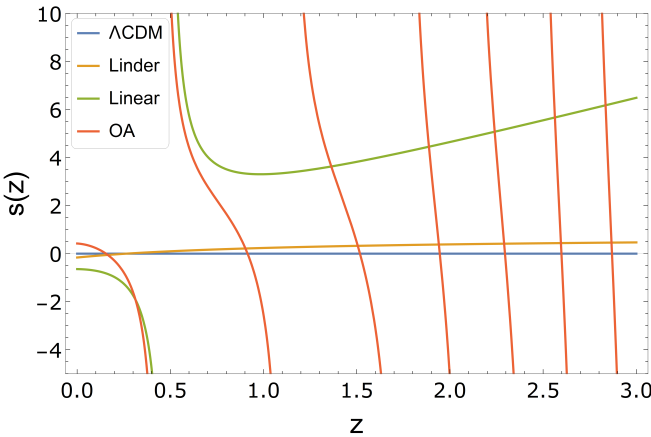


FIG. 6. Second statefinder parameter versus redshift for the Λ CDM (blue line), Linder (orange line), Linear (green line) and Oscillating Ansatz (red line) models.

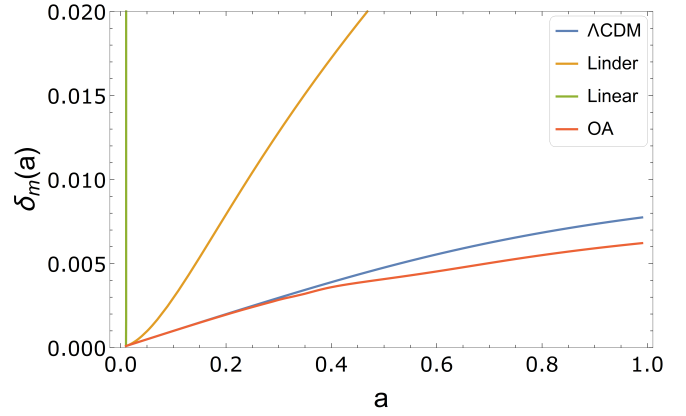


FIG. 7. Matter density perturbation versus the scale factor for the Λ CDM (blue line), Linder (orange line), Linear (green line) and Oscillating Ansatz (red line) models.

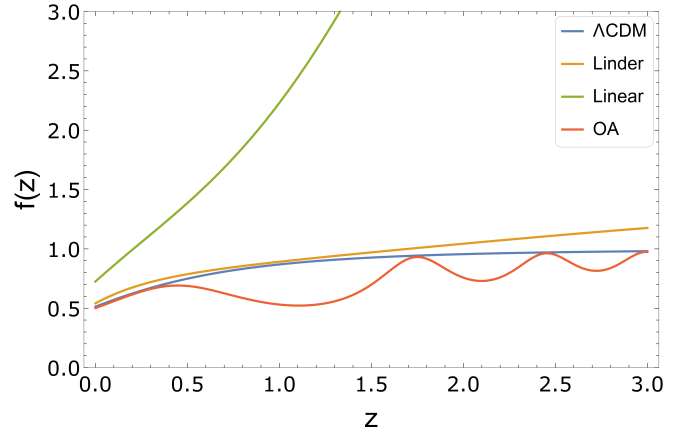


FIG. 8. Growth rate versus redshift for the Λ CDM (blue line), Linder (orange line), Linear (green line) and Oscillating Ansatz (red line) models.

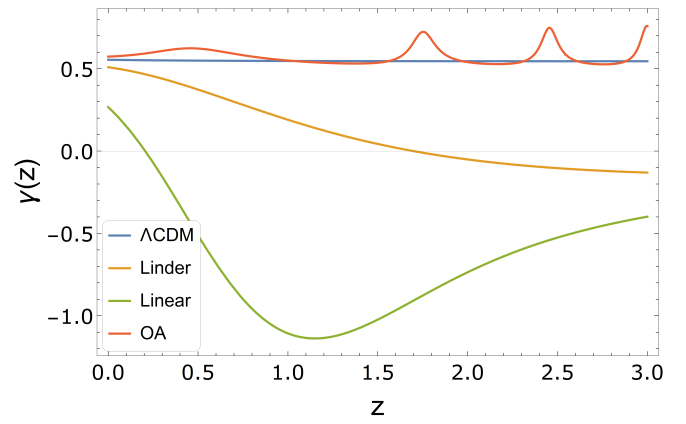


FIG. 9. Growth index versus redshift for the Λ CDM (blue line), Linder (orange line), Linear (green line) and Oscillating Ansatz (red line) models.

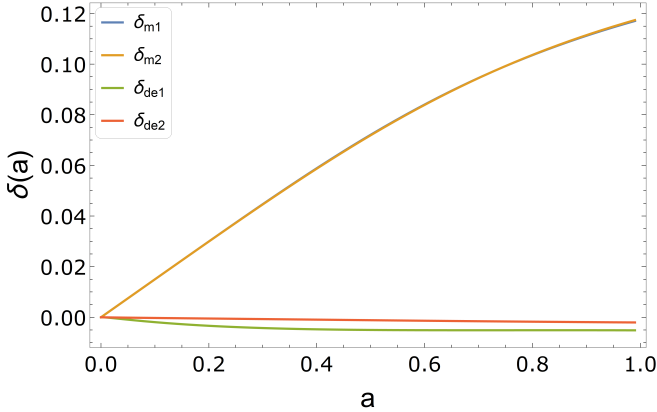


FIG. 10. Matter and DE perturbations versus the scale factor for ODE1 and ODE2 models.

4. CONCLUSIONS

We have discussed different dark energy parametrizations both at background and linear perturbations level and we compared them with the standard cosmological model. We used the parameters that better fits to cosmological data. Using *Mathematica*, we have computed the Hubble and decelerating parameter, as well as the statefinder parameters r, s . We have integrated numerically the evolution of linear perturbation equations and then we obtain the growth rate f , growth index γ . Then we explore a linear growth index parametrization and we compute the equation of state parameter w and the decelerating parameter q .

At a background evolution level, we can only see an agreement between Linder model and Λ CDM model since both shows similar expansion histories. While all models agree on the present value of the deceleration parameter q_0 and the first statefinder parameter r_0 , we can establish

significant differences regarding the present value of the second statefinder parameter s_0 at the present time: s_0 changes between positive, zero and negative values.

At a cosmological perturbation level, we solve the equations for δ in two scenarios: homogeneous dark energy component ($\delta_{de} = 0$) for the first 4 models and when dark energy and matter fully clusters for oscillating dark energy models. In the first scenario we see a better agreement between the oscillating model and Λ CDM model. Matter density perturbations match between OA and Λ CDM models at high redshift, while the Linear model diverges in both matter perturbations and growth rate f . In the second scenario we see a perfect agreement in δ_m for the two oscillatory models even when δ_{de} evolves differently.

Then, we assume some linear function for $\gamma(z)$ as a solution for δ , and we compute the equation of state parameter w and decelerating parameter q . We found a pattern where all curves intersect in the same point and if we plot q_0 versus γ'_0 , the points fits very well a linear function. Then, for $\gamma_0 = 0.55$ and $\gamma'_0 = -0.04$, which are values constrained by measurements of standard sirens, we solve the equation for $F(a)$ and we fit several polynomials, which can be viewed as a Padé parametrization for w . The solution for w represents a quintom model crossing the $w = -1$ line. We found that, unlike previous works, we need to go at least (4, 4) order of the Padé approximation to reach less than 5% error between the numerical value and the fit.

ACKNOWLEDGMENTS

We thank Grigoris Panotopoulos from Centro de Astrofísica e Gravitação, Instituto Superior Técnico-IST, Universidade de Lisboa-UL and Professor Luis Campusano from the Astronomy Department of University of Chile, for reviewing and discussing fundamental ideas in the development of the paper.

-
- [1] Mehdi Rezaei, Mohammad Malekjani, Spyros Basilakos, Ahmad Mehrabi, and David F. Mota. Constraints to dark energy using PADE parameterisations. *arXiv e-prints*, page arXiv:1706.02537 (2017).
 - [2] S. Nesseris and L. Perivolaropoulos. Comparison of cosmological models using recent supernova data. *Phys. Rev. D*, 70, 043531 (2004).
 - [3] Grigoris Panotopoulos and Ángel Rincón. Growth index and statefinder diagnostic of oscillating dark energy. *Phys. Rev. D*, 97, 103509 (2018).
 - [4] David Polarski and Radouane Gannouji. On the growth of linear perturbations. *Physics Letters B*, 660, 439 (2008).
 - [5] Stephen M. Feeney, Hiranya V. Peiris, Andrew R. Williamson, Samaya M. Nissanke, Daniel J. Mortlock, Justin Alsing, and Dan Scolnic. Prospects for Resolving the Hubble Constant Tension with Standard Sirens. *Phys. Rev. Lett.*, 122, 061105 (2019), February 2019.
 - [6] Grigoris Panotopoulos and Ángel Rincón. Model comparison using supernovae and Hubble parameter data. *European Physical Journal Plus*, 134, 354 (2019).
 - [7] S. Nesseris and L. Perivolaropoulos. Testing Λ CDM with the growth function $\delta(a)$: Current constraints. *Phys. Rev. D*, 77, 023504 (2008).
 - [8] Juan Magaña, Víctor H. Cárdenas, and Verónica Motta. Cosmic slowing down of acceleration for several dark energy parametrizations. , 2014, 017 (2014).
 - [9] Imanol Albarran, Mariam Bouhmadi-López, and João Moraes. Cosmological perturbations in an effective and genuinely phantom dark energy Universe. *Physics of the Dark Universe*, 16, 94 (2017).
 - [10] Dragan Huterer and Daniel L. Shafer. Dark energy two decades after: observables, probes, consistency tests. *Reports on Progress in Physics*, 81, 016901 (2018).

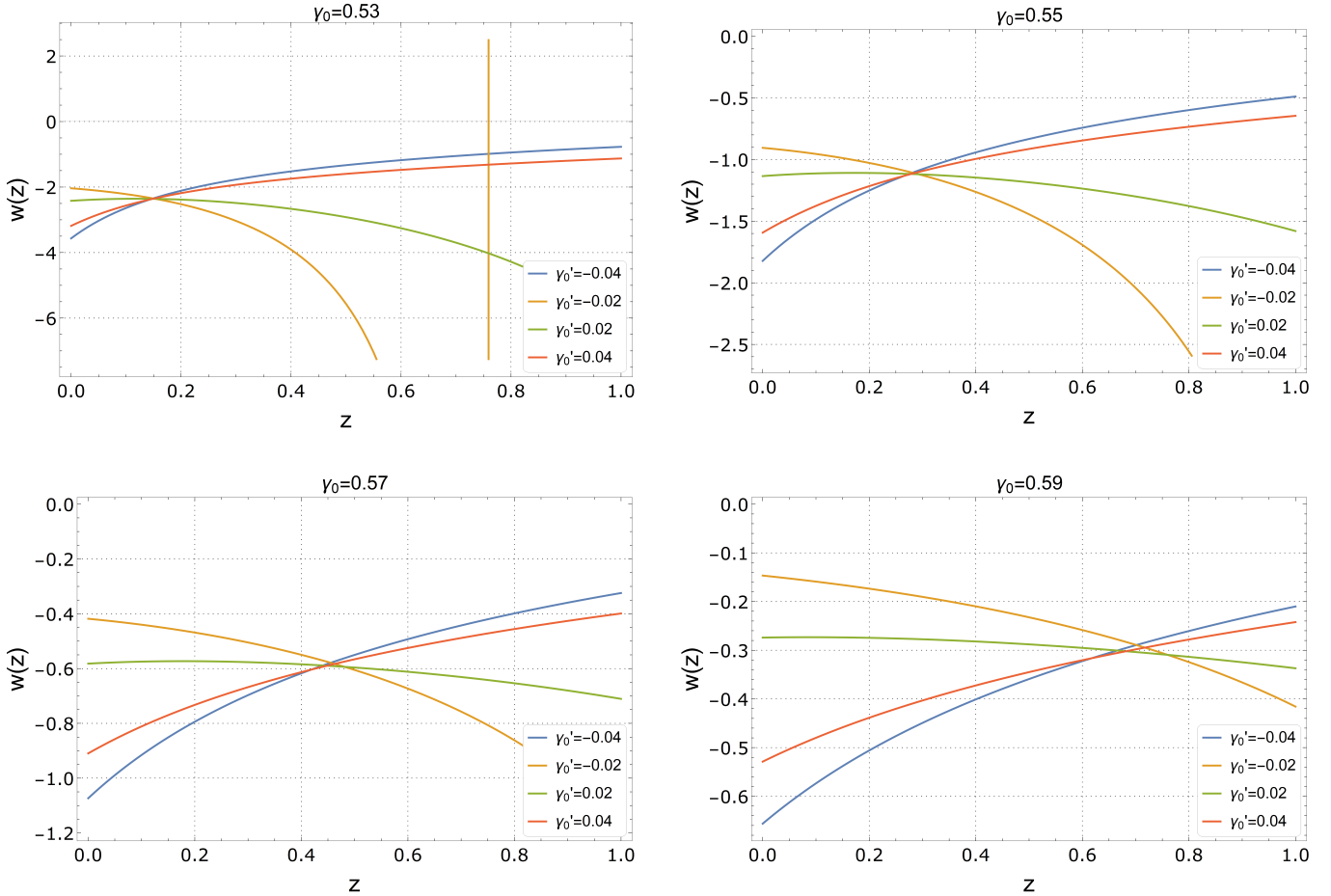


FIG. 11. Equation of state parameter versus redshift for $\gamma(z) = \gamma_0 + \gamma'_0 z$ parametrization.

- [11] Larentios Kazantzidis and Leandros Perivolaropoulos. Evolution of the $f\sigma_8$ tension with the Planck15 / Λ CDM determination and implications for modified gravity theories. *Phys. Rev. D*, 97, 103503 (2018).
- [12] Ahmad mehrabi and Spyros Basilakos. Dark energy reconstruction based on the Padé approximation; an ex-

- pansion around the Λ CDM. *European Physical Journal C*, 78, 889 (2018).
- [13] M. R. Setare and E. N. Saridakis. Quintom dark energy models with nearly flat potentials. *Phys. Rev. D*, 79, 043005 (2009).

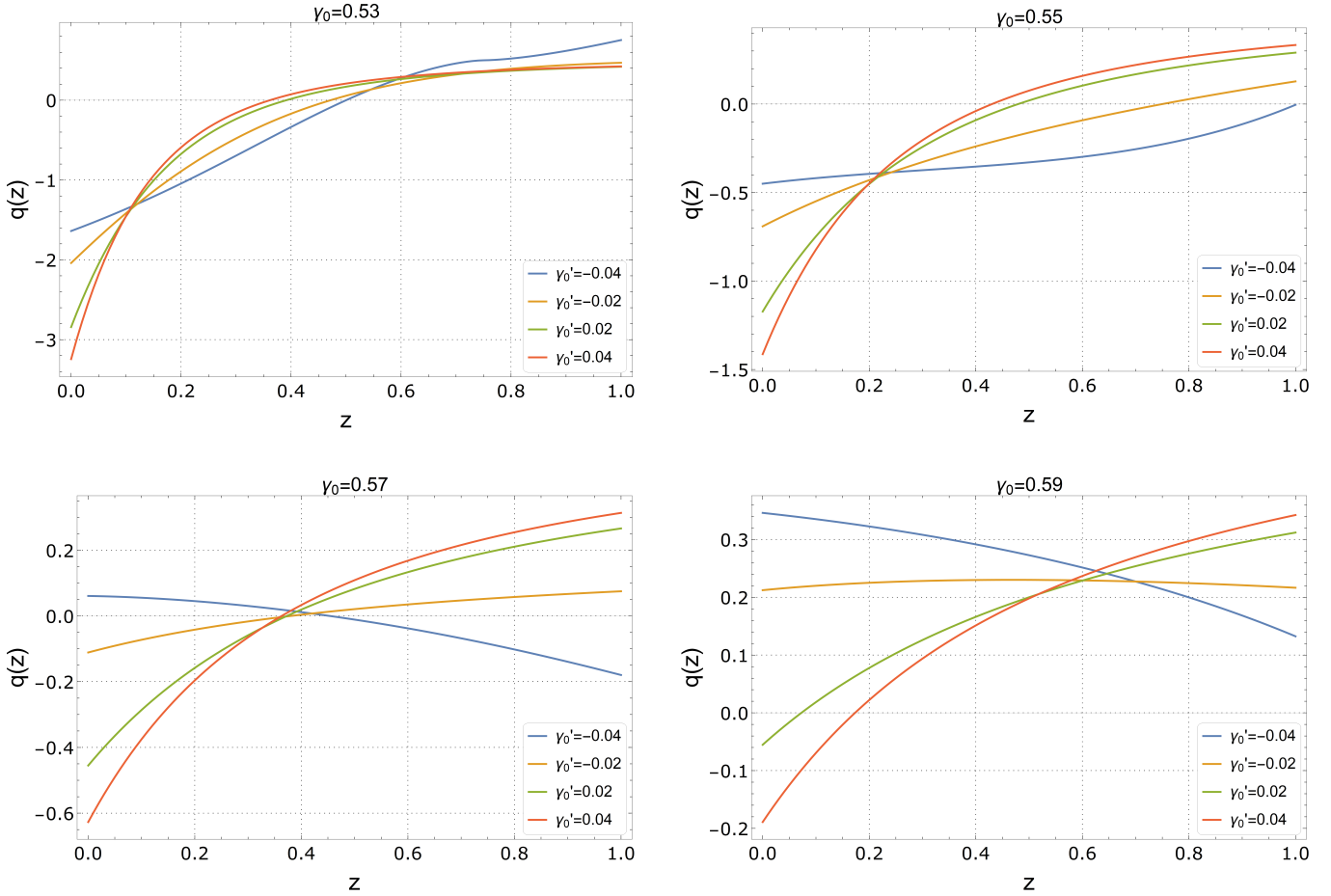


FIG. 12. Decelerating parameter versus redshift for $\gamma(z) = \gamma_0 + \gamma'_0 z$ parametrization.

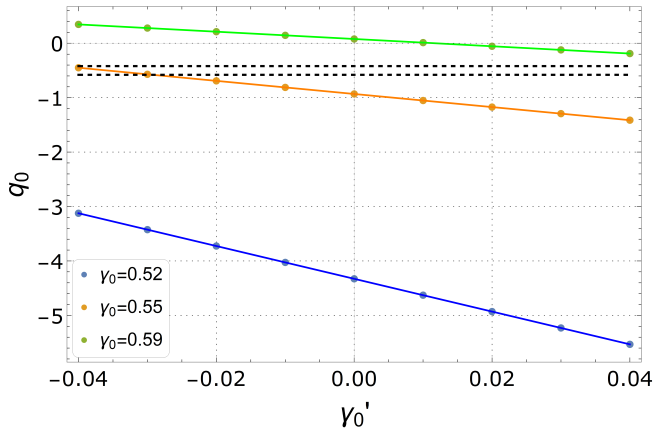


FIG. 13. Decelerating parameter today q_0 versus γ'_0 for $\gamma_0 = 0.52$ (blue dots), $\gamma_0 = 0.55$ (orange dots), $\gamma_0 = 0.59$ (green dots) and its respectively linear fits in color lines. The black-dashed lines represents the $q_0 = -0.5 \pm 0.08$ range.

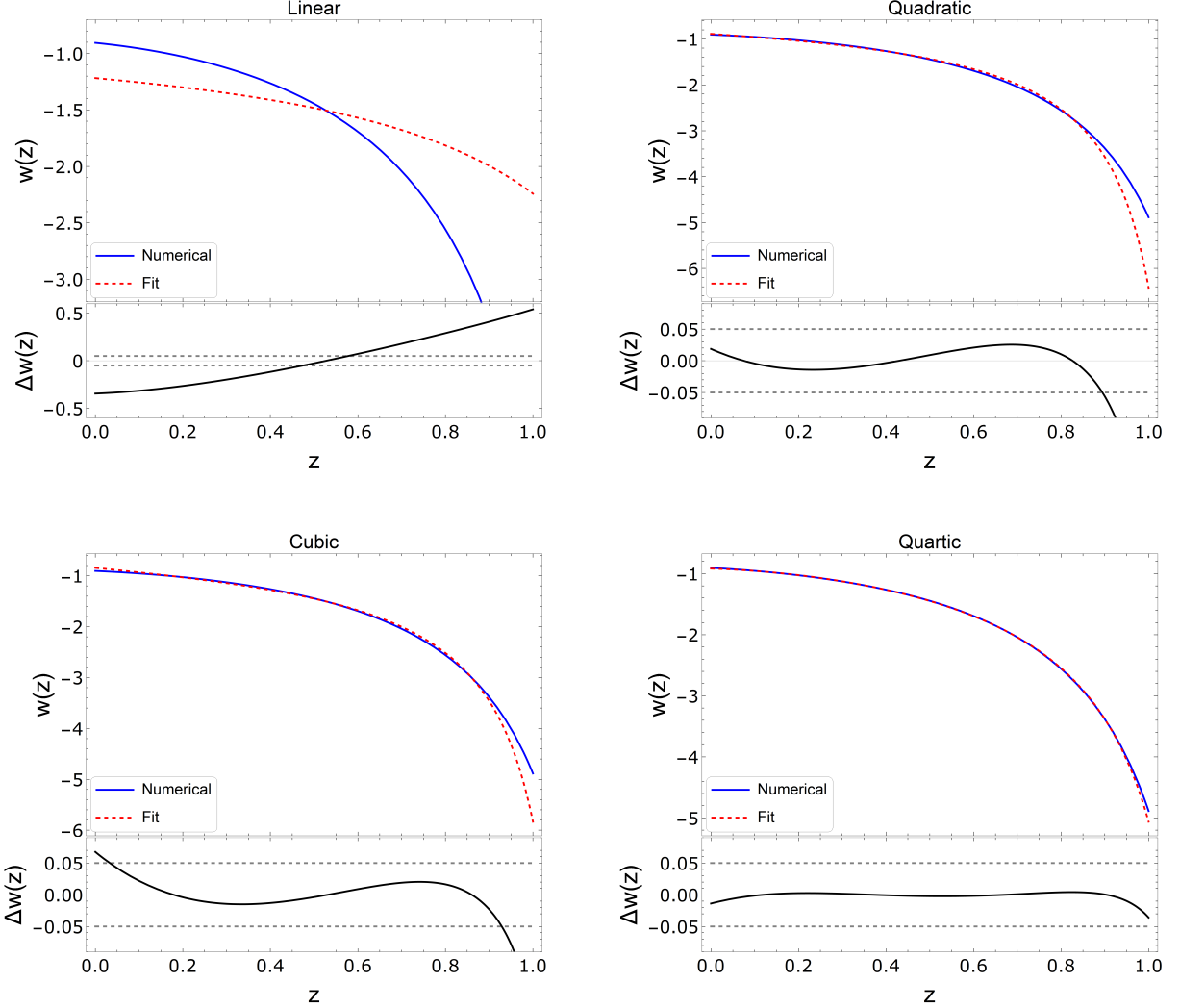


FIG. 14. Top panels: Numerical (blue line) and best polynomial fit equation of state parameter versus redshift (red line). Bottom panels: relative error between the numerical value and the polynomial fit. The gray-dashed lines represents 5% error.